

Field-induced lattice staircase in a frustrated antiferromagnet  $\text{CuFeO}_2$ 

N. Terada,<sup>1</sup> Y. Narumi,<sup>2</sup> K. Katsumata,<sup>1</sup> T. Yamamoto,<sup>3</sup> U. Staub,<sup>4</sup> K. Kindo,<sup>2</sup> M. Hagiwara,<sup>3</sup> Y. Tanaka,<sup>1</sup> A. Kikkawa,<sup>1</sup> H. Toyokawa,<sup>5</sup> T. Fukui,<sup>2</sup> R. Kanmuri,<sup>3</sup> T. Ishikawa,<sup>1</sup> and H. Kitamura<sup>1</sup>

<sup>1</sup>RIKEN Spring-8 Center, Harima Institute, Sayo, Hyogo 679-5148, Japan

<sup>2</sup>ISSP, University of Tokyo, Kashiwa, Chiba 277-8581, Japan

<sup>3</sup>KYOKUGEN, Osaka University, Toyonaka, Osaka 560-8531, Japan

<sup>4</sup>Swiss Light Source, Paul Scherrer Institut, 5232 Villigen, Switzerland

<sup>5</sup>Spring-8/JASRI, Sayo, Hyogo 679-5198, Japan

(Received 18 October 2006; published 20 November 2006)

The results of synchrotron x-ray diffraction and magnetization measurements on a triangular lattice antiferromagnet  $\text{CuFeO}_2$  subjected to a pulsed high magnetic field are reported. We find the lattice constant,  $b$ , contracts stepwise with increasing magnetic field in coincidence with the multistep magnetization changes. These changes in the lattice constant scale with the magnetization changes. We argue that the competition among the ferromagnetic direct and antiferromagnetic superexchange interactions is a main source for this phenomenon. With the changes of the magnetic structure under an applied magnetic field, the number of up spins increases and the lattice contracts to gain the former exchange energy.

DOI: 10.1103/PhysRevB.74.180404

PACS number(s): 75.80.+q, 61.10.Nz, 75.25.+z, 75.30.Kz

The discovery of new electronic properties, including high-temperature superconductivity, the colossal magnetoresistance effect, and multiferroic modifications has fueled a resurgence of work on the complex interplay between charge, spin, orbital, and lattice degrees of freedom.

The compound  $\text{CuFeO}_2$  (abbreviated CFO hereafter) is an antiferromagnet on a triangular lattice and has been studied extensively in the last 15 years.<sup>1–11</sup> In an antiferromagnet on a triangular lattice, one expects to find exotic magnetic properties such as successive phase transitions, noncollinear magnetic structures, and so on, due to the geometrical frustration. Recently, Kimura *et al.* reported the observation of ferroelectricity under applied magnetic fields in CFO,<sup>10</sup> which could be explained by the newly developed theories on multiferroics.<sup>12,13</sup> In this Rapid Communication, we report the observation of stepwise lattice distortions associated with the field induced multistep magnetization changes in CFO.

CFO has the delafossite structure (space group  $R\bar{3}m$ ) at room temperature and the lattice constants are  $a=3.03$  Å and  $c=17.09$  Å. The structure consists of  $\text{Fe}^{3+}$  hexagonal layers along the  $c$  axis, which are separated by intervening two layers of oxygen and one layer of  $\text{Cu}^{1+}$ . Therefore CFO is an ideal system to study the magnetism on a triangular lattice.

Figure 1 shows a schematic phase diagram of CFO in the temperature,  $T$ , versus applied magnetic field,  $B$ , plane. At  $T_{N1} \approx 14$  K, CFO undergoes a transition from the paramagnetic to a partially disordered (PD) phase<sup>2</sup> and at  $T_{N2} \approx 11$  K from PD to an antiferromagnetic phase. The magnetic structure in the PD phase has been a subject of debate<sup>1,2,5,8</sup> and has been finally determined to be a sinusoidally amplitude modulated one. The magnetic structure below  $T_{N2}$  is a collinear four-sublattice one in which spins point along the  $c$  axis and are arranged in a  $\uparrow\uparrow\downarrow\downarrow$  sequence along the hexagonal  $[1\ 1\ 0]$  direction.<sup>1,2</sup> When placed in an applied magnetic field, CFO exhibits successive magnetic transitions below  $T_{N2}$  as evidenced by magnetization changes<sup>3,4</sup> at  $B_{c1} \approx 7$  T,  $B_{c2} \approx 13$  T,  $B_{c3} \approx 20$  T,  $B_{c4} \approx 34$  T, and  $B_{c5} \approx 70$  T. At  $B_{c1} < B < B_{c2}$ , the spin structure is an in-

commensurate one and at  $B_{c2} < B < B_{c3}$  a collinear five-sublattice structure,  $\uparrow\uparrow\downarrow\downarrow$ , is realized.<sup>6</sup> The magnetic structures in the high field phases at  $B_{c3} < B < B_{c4}$  and  $B_{c4} < B < B_{c5}$  have not been determined. As is seen from our magnetization data presented in Fig. 2, CFO exhibits a plateau at  $B_{c3} < B < B_{c4}$  with a magnetization  $\approx 1.6\mu_B/\text{Fe}$ , which is one-third of the saturation value of  $5\mu_B/\text{Fe}$ .<sup>3</sup> Then, we may assume a collinear  $\uparrow\uparrow\downarrow$  structure in this field range. Above  $B_{c4}$  the magnetization seems to increase monotonically with increasing  $B$  and becomes saturated at  $B_{c5} \approx 70$  T.<sup>3</sup>  $\text{Fe}^{3+}$  in CFO is in an orbital singlet state with spin,  $S=5/2$ .<sup>2</sup> Therefore the magnetic properties of CFO should be understood in terms of a Heisenberg model with weak Ising anisotropy. Theory predicts that a Heisenberg antiferromagnet on the triangular lattice with Ising anisotropy exhibits a successive magnetic transition in zero field and an appearance of the  $\uparrow\uparrow\downarrow$  magnetic structure in the intermediate field range at low temperatures.<sup>14</sup> The theory also predicts that at the higher fields above the three-sublattice  $\uparrow\uparrow\downarrow$  phase, spins on the up

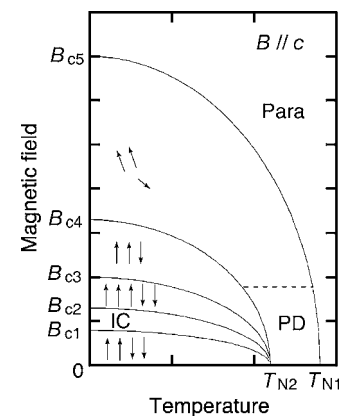


FIG. 1. Schematic temperature vs magnetic field phase diagram of  $\text{CuFeO}_2$  when the external magnetic field  $B$  is applied along the  $c$  axis. Para: paramagnetic phase, PD: partially disordered phase, and IC: incommensurate phase. Arrows show magnetic moments.

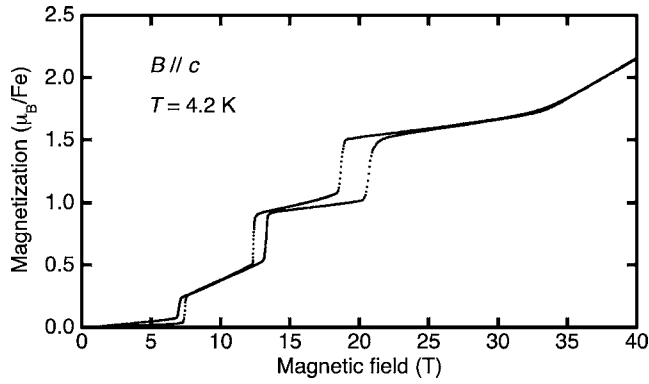


FIG. 2. Magnetic field dependence of the magnetization of  $\text{CuFeO}_2$  measured in pulsed magnetic fields. The external magnetic field is applied along the  $c$  axis.

sublattices are parallel to each other, making an angle with  $\mathbf{B}$ , and the spins on the down sublattice are tilted towards  $\mathbf{B}$  to gain the Zeeman energy as shown schematically in Fig. 1.<sup>14</sup> According to this theory, the ground state spin configuration is the so-called  $120^\circ$  structure in which neighboring spins make an angle  $120^\circ$ . This contradicts with the observation that the low temperature–low field magnetic structure of CFO is the collinear  $\uparrow\uparrow\downarrow\downarrow$  one. Recently, Terada *et al.*<sup>9</sup> and Ye *et al.*<sup>11</sup> reported a structural change in CFO below  $T_{N2}$ . Moreover, Terada *et al.* observed superlattice reflections from which they proposed a scalene triangle model. This local distortion of the triangle partially relieves the frustration and leads to the collinear structure.<sup>9</sup>

Single crystals of CFO were grown by a floating zone method at RIKEN. Synchrotron x-ray diffraction measurements in pulsed high magnetic fields were conducted at the beamline BL19LXU at SPring-8. The data were taken with a PILATUS 100 K detector system, a single photon counting detector.<sup>15</sup> The experimental details are given in Ref. 16. We have made a new magnet (# 4 magnet) for this experiment that has larger inductance compared with the previous ones. In combination with an increase of capacitance, the pulse duration is increased from 5 to 27 ms, which largely improved the statistics of the data. This also makes a precise measurement of field induced phase transitions possible, since the change in magnetic field can be smaller for a given time window. The single crystal was mounted with its  $c$  axis vertical ( $\parallel\mathbf{B}$ ) in a glass dewar that was inserted into the pulsed field magnet. Incident and diffracted x-ray beams were in the horizontal  $ab$  plane ( $\perp\mathbf{B}$ ). The magnetization of the same sample used in the x-ray diffraction study was measured at KYOKUGEN, Osaka University, under pulsed high magnetic fields.

Figure 2 shows the magnetic field dependence of the magnetization of CFO. The external magnetic field is applied along the  $c$  axis. The transitions at  $B_{c1} \approx 7$  T,  $B_{c2} \approx 13$  T, and  $B_{c3} \approx 20$  T show hysteresis indicating that these transitions are of first order. At  $B_{c2} < B < B_{c3}$ , the magnetization is almost independent of  $B$  and the magnitude is about one-fifth of the saturation value. This is expected from the collinear  $\uparrow\uparrow\downarrow\downarrow$  magnetic structure described above. As already discussed above, we have the  $1/3$  magnetization plateau at  $B_{c3} < B < B_{c4}$ .

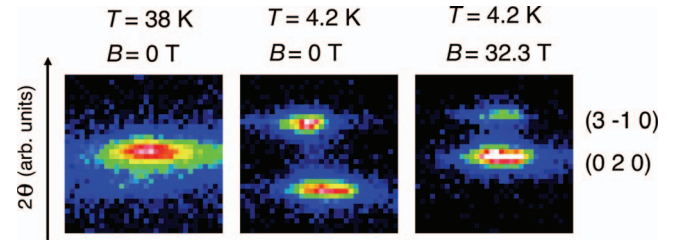


FIG. 3. (Color) X-ray diffraction images obtained at  $T=38$  K and  $B=0$  T (left),  $T=4.2$  K and  $B=0$  T (middle), and at  $T=4.2$  K and  $B=32.3$  T (right).

Since we can access only the Bragg points in the  $ab$  plane in the present synchrotron diffraction measurements, the indexing of the Bragg points is conveniently made based on the orthorhombic unit cell<sup>9</sup>. The relation between the lattice constants in the hexagonal cell ( $a_h, c_h$ ) and the orthorhombic cell ( $a_{\text{orth}}, b_{\text{orth}}, c_{\text{orth}}$ ) is  $a_{\text{orth}} = \sqrt{3}a_h$ ,  $b_{\text{orth}} = a_h$ , and  $c_{\text{orth}} = c_h$ . Figure 3 shows an image of the diffraction taken at the designated temperatures and magnetic fields. We have observed  $(0\ 2\ 0)$  and  $(3\ \bar{1}\ 0)$  Bragg reflections from which we deduce the lattice constants  $a_{\text{orth}}$  and  $b_{\text{orth}}$ .

Figure 4 shows the magnetic field dependence of the lattice constants  $a_{\text{orth}}$  and  $b_{\text{orth}}$  measured at  $T=4.2$  K. We see that the lattice constant  $b_{\text{orth}}$  decreases stepwise with increasing  $B$ . This result is consistent with the macroscopic measurement by Kimura *et al.*, who observed a discontinuous change in the magnetostriction at about 7 and 13 T.<sup>10</sup> In the present study, we demonstrate that the phenomenon occurs in an atomic level. The lattice constant  $a_{\text{orth}}$  increases slightly with  $B$ . In zero field, Terada *et al.* observed that  $a_{\text{orth}}$  contracts, while  $b_{\text{orth}}$  elongates with decreasing temperature below  $T_{N2}$ .<sup>9</sup> Combining the zero field data and the present results, we expect that the scalene triangle becomes an isosceles one with increasing  $B$  and finally an equilateral one above  $B_{c5}$ .

We plot in Fig. 5 a relative change in the magnetization and that in the lattice constant  $b_{\text{orth}}$  as a function of  $B$ . Here, the magnetization is scaled by its saturation value ( $5\ \mu_B/\text{Fe}$ ) and the lattice constant is scaled as  $\alpha[b_{\text{orth}}(B=0\ \text{T}) - b_{\text{orth}}(B)]/b_{\text{orth}}(B=0\ \text{T})$ , where  $\alpha$  is a numerical factor. We

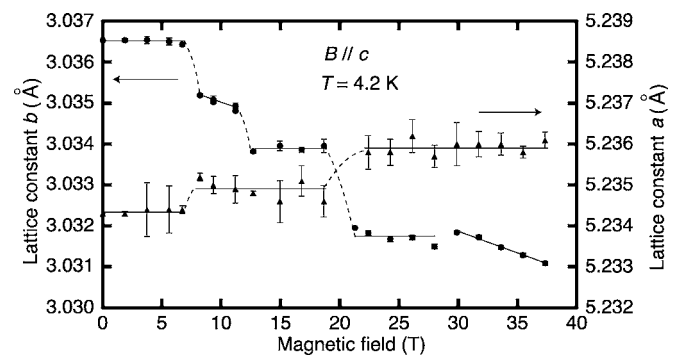


FIG. 4. Magnetic field dependence of the lattice constant  $a_{\text{orth}}$  (filled triangle scaled by the right axis) and  $b_{\text{orth}}$  (filled circle scaled by the left axis) measured at  $T=4.2$  K. The solid lines and dotted curves are drawn as a guide to the eye.

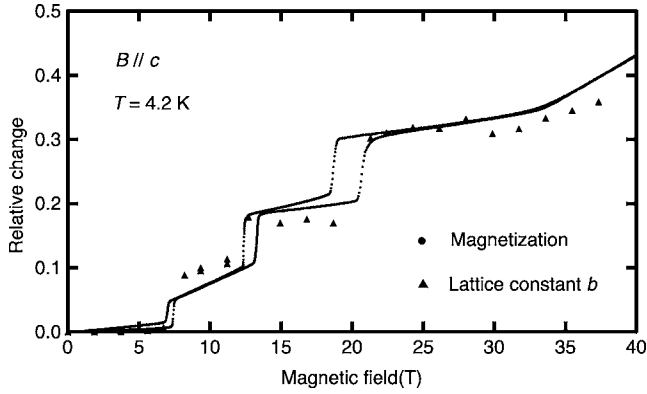


FIG. 5. Magnetic field dependence of the magnetization (filled circle) scaled by its saturation value and the lattice constant  $b_{\text{orth}}$  (filled triangle) scaled as  $\alpha[b_{\text{orth}}(B=0 \text{ T}) - b_{\text{orth}}(B)]/b_{\text{orth}}(B=0 \text{ T})$ , where  $\alpha$  is a numerical factor.

see the two quantities are nicely correlated. To the best of our knowledge, there has been no report on stepwise lattice distortions which are correlated with field induced successive magnetic transitions.

We discuss the origin of the stepwise lattice distortions. In Fig. 6(a) are shown the exchange interaction paths based on the scalene triangle model.<sup>9</sup> In this case, we consider only the nearest neighbor interactions along the three edges of a triangle and further neighbor interactions introduced by Mekata *et al.*<sup>2</sup> are neglected. Figure 6(b) represents the ground state four-sublattice spin structure in the basal plane of CFO determined from the neutron diffraction studies.<sup>1,2</sup> As noted above,  $\text{Fe}^{3+}$  spin in CFO behaves as a Heisenberg one and we treat it as a classical spin, because the spin value is large ( $S = \frac{5}{2}$ ). Writing exchange interaction between spins  $S_i$  and  $S_j$  as  $J_{ij}S_iS_j$  ( $J > 0$  for antiferromagnetic interaction), the energy per spin of the four-sublattice phase at  $T=0 \text{ K}$  is given by

$$-S^2(J'_1 + J'_2 - J'_3), \quad (1)$$

and the corresponding quantity of the 120° structure is

$$-\frac{1}{2}S^2(J'_1 + J'_2 + J'_3). \quad (2)$$

Therefore the four-sublattice state is realized in the ground state if  $(J'_1 + J'_2)/3 > J'_3$ . In a magnetic field applied along the  $c$  axis, the four-sublattice state becomes unstable because this state has no net moment. Then spins will turn their direction from the  $c$  axis making an angle with  $\mathbf{B}$ . The tilted structure has a net moment. This is reflected in the linear increase of the magnetization at  $B_{c1} < B < B_{c2}$ . Because of the Ising anisotropy, this tilted state becomes unstable at higher fields. Then, we expect a collinear spin structure will reappear. Let us start from the  $\uparrow\uparrow\downarrow\downarrow$  state in Fig. 6(b). When we flip the down spins on the third column, we have a  $\uparrow\uparrow\uparrow\downarrow$  state that has a magnetization half the saturation value. Since we have not observed a  $\frac{1}{2}$  plateau in the magnetization curve, this state is not a stable one. Then, we simultaneously flip the spins on the third and fifth columns and obtain the  $\uparrow\uparrow\uparrow\downarrow\downarrow$  state, as observed from neutron diffraction measurement.<sup>6</sup>

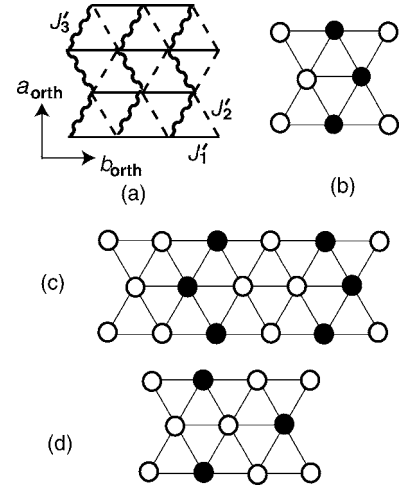


FIG. 6. (a) The exchange interaction paths in the basal plane. (b) The spin structure in the basal plane of the four-sublattice  $\uparrow\uparrow\downarrow\downarrow$  phase. (c) The spin structure in the basal plane of the five-sublattice  $\uparrow\uparrow\uparrow\downarrow\downarrow$  phase. (d) The spin structure in the basal plane of the three-sublattice  $\uparrow\uparrow\downarrow$  phase. Empty and filled circles show up and down spins, respectively. Spins are directed perpendicular to the plane of the paper. Here, (d) is a model structure that can explain the magnetization and the lattice distortion.

Similarly, we obtain the  $\uparrow\uparrow\downarrow$  state from a simultaneous flipping of the third, fourth, fifth, and sixth columns of the  $\uparrow\uparrow\uparrow\downarrow\downarrow$  state. All these changes in spin structure occur along the  $b_{\text{orth}}$  axis, i.e., the  $J'_1$  interaction plays an essential role in the field-induced magnetic phase transitions. This explains why the change in  $a_{\text{orth}}$  with magnetic field is small and the correlation with the magnetization changes is less clear.

As is discussed by Mekata *et al.*,<sup>2</sup> the nearest neighbor exchange interaction in the basal plane of CFO is a sum of the direct exchange interaction, which is assumed to be ferromagnetic, and the 90° superexchange interaction through an  $\text{O}^{2-}$  ion. The latter exchange interaction involves several mechanisms and the sign is uncertain.<sup>17</sup> Kanamori suggested that the 90° superexchange interaction between spins in the  $3d^5$  system would be antiferromagnetic,<sup>17</sup> and we believe this is the case judging from the antiferromagnetic ordering in this compound. The experimental evidence that the  $b$  axis elongates at low temperatures in zero field<sup>9</sup> implies that the direct exchange interaction diminishes and the antiferromagnetic interaction dominates. This stabilized the  $\uparrow\downarrow\uparrow\downarrow$  sequence in the rows of the four-sublattice structure given in Fig. 6(b). In the five-sublattice state, one out of five  $J'_1$  bonds is coupled by two parallel spins and costs energy. In order to lower this cost in the exchange energy,  $b_{\text{orth}}$  axis contracts to resume the ferromagnetic direct exchange interaction. In the three-sublattice phase, one out of three  $J'_1$  bonds is coupled by two parallel spins, so that an additional lattice contraction along the  $b_{\text{orth}}$  axis is needed. In these field-induced lattice changes, we expect that a uniform distortion will occur rather than a local distortion at the “wrong” bonds. This explains qualitatively the stepwise lattice contractions in  $b_{\text{orth}}$  associated with the multistep magnetization changes in CFO.

In conclusion, we have performed synchrotron x-ray diffraction and magnetization measurements on CFO under a pulsed high magnetic field. We find the lattice constant,  $b_{\text{orth}}$ , contracts stepwise with increasing  $B$ . These changes in the lattice constant coincide with the multistep magnetization changes. We find that the lattice changes are scaled with the magnetization changes. We interpreted the result by the competition between the nearest neighbor ferromagnetic direct and antiferromagnetic superexchange interactions. With in-

creasing  $B$ , the number of up spins increases and the lattice contracts to gain the ferromagnetic exchange energy.

N.T. was supported by the Special Researchers' Basic Science Program (RIKEN). This work was supported in part by Grant-in-Aid for Scientific Research on priority Areas "High Field Spin Science in 100T" (No. 451) from the Ministry of Education, Culture, Sports, Science and Technology (MEXT)

- 
- <sup>1</sup>S. Mitsuda, H. Yoshizawa, N. Yaguchi, and M. Mekata, *J. Phys. Soc. Jpn.* **60**, 1885 (1991).
- <sup>2</sup>M. Mekata, N. Yaguchi, T. Takagi, T. Sugino, S. Mitsuda, H. Yoshizawa, N. Hosoito, and T. Shinjo, *J. Phys. Soc. Jpn.* **62**, 4474 (1993).
- <sup>3</sup>Y. Ajiro, T. Asano, T. Takagi, M. Mekata, H. Aruga Katori, and T. Goto, *Physica B* **201**, 71 (1994).
- <sup>4</sup>Y. Ajiro, K. Hanasaki, T. Asano, T. Takagi, M. Mekata, H. Aruga Katori, and T. Goto, *J. Phys. Soc. Jpn.* **64**, 3643 (1995).
- <sup>5</sup>S. Mitsuda, N. Kasahara, T. Uno, and M. Mase, *J. Phys. Soc. Jpn.* **67**, 4026 (1998).
- <sup>6</sup>S. Mitsuda, M. Mase, K. Prokes, H. Kitazawa, and H. Aruga Katori, *J. Phys. Soc. Jpn.* **69**, 3513 (2000).
- <sup>7</sup>O. A. Petrenko, G. Balakrishnan, M. R. Lees, D. McK. Paul, and A. Hoser, *Phys. Rev. B* **62**, 8983 (2000).
- <sup>8</sup>N. Terada, T. Kawasaki, S. Mitsuda, H. Kimura, and Y. Noda, *J. Phys. Soc. Jpn.* **74**, 1561 (2005).
- <sup>9</sup>N. Terada, S. Mitsuda, H. Ohsumi, and K. Tajima, *J. Phys. Soc. Jpn.* **75**, 023602 (2006).
- <sup>10</sup>T. Kimura, J. C. Lashley, and A. P. Ramirez, *Phys. Rev. B* **73**, 220401(R) (2006).
- <sup>11</sup>F. Ye, Y. Ren, Q. Huang, J. A. Fernandez-Baca, P. Dai, J. W. Lynn, and T. Kimura, *Phys. Rev. B* **73**, 220404(R) (2006).
- <sup>12</sup>H. Katsura, N. Nagaosa, and A. V. Balatsky, *Phys. Rev. Lett.* **95**, 057205 (2005).
- <sup>13</sup>M. Mostovoy, *Phys. Rev. Lett.* **96**, 067601 (2006).
- <sup>14</sup>S. Miyashita, *J. Phys. Soc. Jpn.* **55**, 3605 (1986).
- <sup>15</sup>Ch. Broennimann, E. F. Eikenberry, B. Henrich, R. Horisberger, G. Huelsen, E. Pohl, B. Schmitt, C. Schulze-Briese, M. Suzuki, T. Tomizaki, H. Toyokawa, and A. Wagner, *J. Synchrotron Radiat.* **13**, 120 (2006).
- <sup>16</sup>Y. Narumi, K. Kindo, K. Katsumata, M. Kawauchi, Ch. Broennimann, U. Staub, H. Toyokawa, Y. Tanaka, A. Kikkawa, T. Yamamoto, M. Hagiwara, T. Ishikawa, and H. Kitamura, *J. Synchrotron Radiat.* **13**, 271 (2006).
- <sup>17</sup>J. Kanamori, *J. Phys. Chem. Solids* **10**, 87 (1959).